

## RESEARCH

# Detection accuracy of condylar bony defects in Promax 3D cone beam CT images scanned with different protocols

Z-L Zhang<sup>1</sup>, J-G Cheng<sup>1</sup>, G Li<sup>\*1</sup>, X-Q Shi<sup>2</sup>, J-Z Zhang<sup>3</sup>, Z-Y Zhang<sup>1</sup> and X-C Ma<sup>\*1</sup>

<sup>1</sup>Department of Oral and Maxillofacial Radiology, Peking University School and Hospital of Stomatology, Beijing, China;

<sup>2</sup>Department of Oral Radiology, Karolinska Institutet, Stockholm, Sweden; <sup>3</sup>Department of Forensic Pathology and Anthropology, Institute of Forensic Sciences, Ministry of Public Security P.R.C., Beijing, China

**Objectives:** To investigate and compare the detection accuracy of bony defects on the condylar surface of the temporomandibular joint (TMJ) in cone beam CT (CBCT) images scanned with standard and large view protocols on the same machine.

**Methods:** 21 dry human skulls with 42 TMJs were scanned with the large view and standard view protocols of the CBCT scanner Promax 3D (Planmeca, Helsinki, Finland). Seven observers evaluated all the images for the presence or absence of defects on the surface of the condyle. Using the macroscopic examination of condylar defects as the gold standard, receiver operating characteristic (ROC) analysis was performed.

**Results:** Macroscopic examination revealed that, of the 42 condyles, 18 were normal and 24 had a defect on the surface of the condyles. Areas under the ROC curves for the large view and the standard view group of CBCT images were 0.739 and 0.720, respectively, and no significant difference was found between the two groups of images ( $p = 0.902$ ). Neither the interobserver nor the intraobserver variability were significant.

**Conclusions:** The two scanning protocols provided by the CBCT scanner Promax 3D were reliable and comparable with detection of condylar defects.

*Dentomaxillofacial Radiology* (2013) **42**, 20120241. doi: 10.1259/dmfr.20120241

**Cite this article as:** Zhang Z-L, Cheng J-G, Li G, Shi X-Q, Zhang J-Z, Zhang Z-Y, et al. Detection accuracy of condylar bony defects in Promax 3D cone beam CT images scanned with different protocols. *Dentomaxillofac Radiol* 2013; **42**: 20120241.

**Keywords:** temporomandibular joint; mandibular condyle; radiology; cone beam computed tomography

## Introduction

Conventionally, the most commonly used radiographic methods for the evaluation of osseous changes of the temporomandibular joint (TMJ) include panoramic radiography, tomography, transpharyngeal or transcranial projections. With the introduction of CT, the osseous components of the TMJ can be viewed three-dimensionally. It was reported that, for degenerative arthritis of the TMJ, the detection accuracy represented by the percentage of the joint with

a correct diagnosis (true-positive and true-negative diagnosis) can reach 87.5–96.0% with the application of CT imaging.<sup>1,2</sup> Unfortunately, most CT units are large and expensive, and are not readily available to dentists.

Cone beam CT (CBCT) is a newly developed technique that can provide three-dimensional hard-tissue images of the oral and maxillofacial regions. Because of its lower radiation dose,<sup>3</sup> higher spatial resolution<sup>4</sup> and easy access when compared with multislice CT, it has been widely accepted and used for different diagnostic tasks including oral surgery, oral medicine, endodontics, periodontology, orthodontics and implantology.<sup>5–9</sup> The technique can also provide a complete radiographic investigation of the bony components of the

\*Correspondence to: G Li or X-C Ma, Department of Oral and Maxillofacial Radiology, Peking University School and Hospital of Stomatology, #22 Zhongguancun Nandajie, Hai Dian District, Beijing 100081, China. E-mail: [kqgang@bjmu.edu.cn](mailto:kqgang@bjmu.edu.cn) or [kqxcma@bjmu.edu.cn](mailto:kqxcma@bjmu.edu.cn)

The study is supported by Capital Research Fund for Medical Development. Received 1 July 2012; revised 27 September 2012; accepted 1 October 2012

TMJ.<sup>10–13</sup> Recent studies have revealed that CBCT is a reliable alternative to multislice CT for the assessment of the TMJ space and osseous changes.<sup>14,15</sup>

For the purposes of different diagnostic tasks and minimizing the radiation dose to patients, nowadays CBCT scanners allow users to select the field of view (FOV), high- or low-spatial resolution and patient size when scanning a patient. A recent study has indicated that, when applying different dental protocols, the effective radiation doses of the CBCT scanner Promax 3D (Planmeca, Helsinki, Finland) are quite different.<sup>16</sup> For example, when scanning the TMJs with a combination of a full FOV of 8×8 cm, the largest patient size and a normal resolution given a voxel size of 0.32 mm and 12 bit pixel depth, a protocol that will be called standard view hereafter, the effective radiation dose of one scan is 298  $\mu$ Sv; however, when using the large view protocol, which combines three full FOVs horizontally by stitching, a method used to correct and register the spatial orientation of the three volumes and align them to one another, the effective radiation dose is 87  $\mu$ Sv for both TMJs, which is only about one-third of that when applying the standard view protocol.<sup>16</sup>

If both TMJs are examined with a single scan using the large view protocol, the effective radiation dose will be considerably reduced. However, in theory, a low dose results in a low signal-to-noise ratio and consequently a low diagnostic image quality. The purpose of the present study was therefore to evaluate and compare the osseous changes of the TMJ in the Promax 3D CBCT images scanned with the standard and the large view protocols.

## Materials and methods

### *Skulls and gold standard*

42 joints in 21 dry human skulls were employed. These skulls were supplied by the Institute of Forensic Sciences, Ministry of Public Security, China. The selection criteria were as described in a previous study.<sup>17</sup> Because we used dry human skulls in the study, ethics approval by the institutional review board was not necessary.

The appearances of the condylar surfaces ranged from normal to having a defect of varying size. The macroscopic definition of the bony defect, which was only used to determine the presence or absence of bony defects and not for statistical analysis in the present study, was: (1) destructive and erosive osseous changes of the condyle, (2) flattening of the articular surface of the condyle and (3) deformity of the condyle. To determine the presence or absence of bony defects, all condyles were viewed by two investigators. The following two-point scale was used to score the status of the condylar surfaces: 0 = absence of bony defect and 1 = at least one bony defect present on the condylar surface. In cases where the investigators' ratings

diverged, a joint assessment was performed until consensus was reached. An example image of a condyle is shown in [Figure 1a](#).

### *CBCT images*

CBCT images of the 42 TMJs were acquired with the CBCT scanner Promax 3D, which can provide different scanning protocols by combining patient size, volume size and image resolutions. The two protocols that are suitable for TMJ examinations were selected. One is called the standard view protocol in this study and the other is the large view protocol that is used to combine three volumes of full FOV horizontally. When the standard view protocol was used for scanning, two scans were performed, one for each TMJ. However, when the large view protocol was applied, only a single scan was needed. The exposure parameters for each scan in this study are presented in [Table 1](#). During the CBCT exposures, a 20 mm thick water phantom was placed around the skull to simulate soft tissue.<sup>17</sup>

To keep the TMJ space stable at its centric occlusion position, an autopolymerizing acrylic resin (Meliodent; Heraeus Kulzer, Hanau, Germany) was used. This acrylic resin was mixed using a ratio (powder to liquid) of 10:7 (w/w). About 5 min later, the mixture was put into both the glenoid fossas of one skull and the associated mandible was positioned to achieve its centric occlusion until the acrylic resin became rigid. Bone surfaces had been coated by a separate liquid before fixation. Adhesive tape was used to ensure fixation of the mandible to the skull throughout the study.

### *Viewing*

Seven resident doctors of dentistry viewed all the images, which were displayed on a 22 inch (56 cm) Dell™ E228WFP flat panel monitor (Dell, Round Rock, TX) with a resolution of 1680 × 1050 pixels. To avoid any possible bias, the two investigators who had determined the bony defect were excluded from the observation of images. The CBCT images were viewed in a blind and random manner with the proprietary software (Romexis® 2.3.0., Planmeca, Helsinki, Finland). The observers were allowed to adjust the brightness and contrast at will and evaluated the images in the axial, coronal and sagittal planes with respect to TMJ condylar bony defects ([Figures 1b,c](#)). Before viewing, each observer was informed on the use of CBCT proprietary software and the definition of a radiological TMJ condylar defect. The radiological condylar defect was defined as (1) faceting—a small, smooth, flat surface or irregularity seen on the bony outline of the condyle producing a sharp deviation in condylar form, (2) lack of cortical definition—loss of peripheral opaque rim of cortical bone or (3) both faceting and lack of cortical contour.<sup>18</sup> This definition was only used to determine the presence or absence of radiological condylar bony defects and not for the statistical analysis. Viewing was conducted in a quiet room with dim light. Each observer

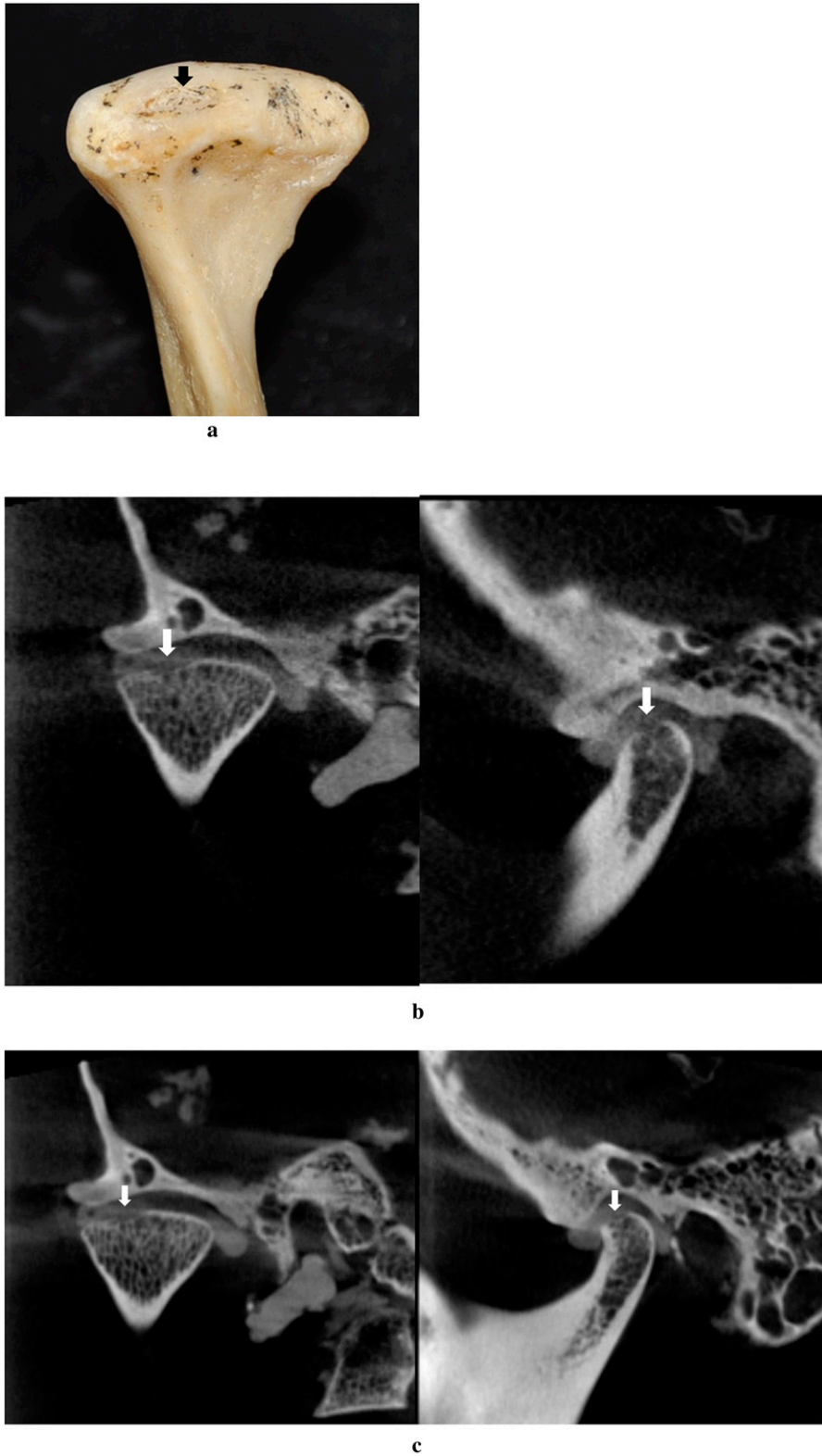


**Figure 1** (a) An example of a condylar defect (solid black arrow). (b) An example of cone beam CT images acquired with the large view protocol. (c) An example of cone beam CT images acquired with the standard view protocol

**Table 1** Specifications of different imaging groups when taking radiographs

Protocol	kV	mAs	Exposure time (s)	Voxel size (mm)	Field of view (mm)	Slice thickness (mm)
Large view	84	6	8.5	0.32	150 × 110 × 80	0.96
Standard view	84	12	12	0.32	80 × 80 × 80	0.96

evaluated only one group of test images at a time. There was a 1 week interval between the adjacent evaluations of large view and standard view images. To investigate the intraobserver agreement, each observer reassessed the images 2 weeks later.

The observers used the following five-point ranking to record their level of confidence with regard to the absence or presence of condylar bony defects: 1 = definitely not present, 2 = probably not present, 3 = uncertain, 4 = probably present and 5 = definitely present.

#### Data analyses

With the macroscopic anatomy examination as the reference standard, each observer's performance was converted into a receiver operating characteristic (ROC) curve with SPSS<sup>®</sup> v. 16.0 for Windows (SPSS, Chicago, IL). The maximum likelihood parameters were determined and the areas under the ROC curves (Az values) were calculated. The t-test was used to analyse the Az values for the differences between imaging groups. One-way analysis of variance was used to analyse the Az values for the differences among observers. Intraobserver variation was analysed with the Wilcoxon test. Differences were considered to be statistically significant when  $p < 0.05$ .

## Results

Macroscopic anatomy examination revealed that, of the 42 TMJ condylar surfaces, 18 (42.86%) were normal and 24 (57.14%) had defects. Thus, 24 condylar surfaces were considered to be positive for a defect when performing the ROC analysis. Table 2 shows the Az values from each observer. There was no statistical difference in

**Table 2** Areas under the receiver operating characteristic curve (Az) obtained from each observer

Observer	Large view	Standard view
1	0.736	0.692
2	0.773	0.675
3	0.688	0.703
4	0.803	0.778
5	0.747	0.705
6	0.683	0.723
7	0.744	0.764
Mean	0.739	0.720
SD	0.043	0.038

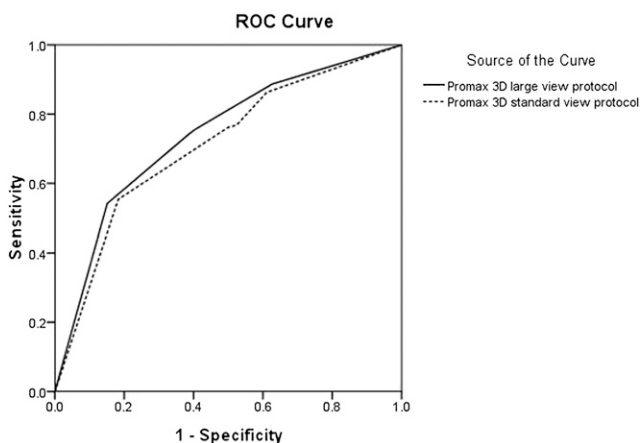
SD, standard deviation.

Az values between the two imaging groups ( $p = 0.902$ ). Figure 2 shows the ROC curves from the pooled observer performances. The ROC curve for the large view protocol images is slightly higher than that for the standard view protocol images. There was no statistically significant difference among (interobserver,  $p = 0.216$ ) or within (intraobserver,  $p = 0.157$ – $0.778$ ) observers.

## Discussion

Because of the potential risk of radiation to patients, the radiation dose of CBCT is a major concern. To minimize the radiation dose without compromising image quality, many scanning protocols have been devised. Combining two or three full FOVs horizontally or vertically for a large view is one such protocol. The present study demonstrated that the detection accuracy of condylar defects represented by the area under the ROC curve was equally good for both the standard and the large view group of images, *i.e.* the images scanned with one full FOV and the images obtained with horizontal stitching of three full FOVs. This implies that, by using the large view protocol to scan a patient for observation of osseous changes of the condyle, the radiation dose can be considerably reduced without any loss of diagnostic accuracy in the images.

In a search of the literature, we did not find any study exclusively focused on the impact of stitching images on the observation of TMJ bony defects. However, several studies were reported with regard to

**Figure 2** Receiver operating characteristic (ROC) curve from the pooled observer performances for each imaging group when the condylar defect was detected

the usefulness of CBCT images in the evaluation of TMJ bone erosions.<sup>10–13,19</sup> In one study, the diagnostic efficacy of condylar erosions was assessed with CBCT images scanned with different voxel sizes and FOVs. In this study, the CBCT scanner CB MercuRay (Hitachi Medical, Twinsburgh, OH) was used and the CBCT images were acquired with a 15 cm FOV at a voxel size of 0.2 mm, a 22.5 cm FOV at a voxel size of 0.3 mm and a 30 cm FOV at a voxel size of 0.4 mm. The results show that, for assessment of bony erosions, the CBCT images acquired with a 15 cm FOV were significantly better than images acquired with a 30 cm FOV.<sup>11</sup> The referenced study shows the effect of FOV and voxel sizes on the critical evaluation of TMJ erosions. In the present study, however, the voxel size and the FOV used to scan a patient was the same for both protocols. The report that is most closely related to the present study is the measurement accuracy of TMJ space distances in CBCT images scanned with the stitching program.<sup>17</sup> In that study, the CBCT scanner Promax 3D was used and the standard and the large view protocols were employed for scanning as well. The results demonstrate that the two scanning protocols were reliable and similar for recording the TMJ space.

The use of dry skulls may be a drawback of the study. However, the studies performed by Li *et al*<sup>20</sup> and Hintze and Wenzel<sup>21</sup> have demonstrated that there is no significant differences between the diagnostic accuracy of

caries obtained both under laboratory conditions and from real patients. One limitation of the present study was the fact that only condylar defects of human dry skull were assessed. These defects occurred naturally or were induced during use. We did not evaluate other bony changes of the TMJ such as osteophytes due to the limited number of such osseous abnormalities in the studied samples.

## Conclusion

Standard view and large view scanning protocols provided by the CBCT scanner Promax 3D were reliable and comparable for detection of TMJ bony defects in dry human skulls. Considering that the two scanning protocols can provide a similar measurement accuracy of the TMJ space and the effective radiation dose obtained from a large view protocol is only about one-sixth of that of two standard view protocols, the large view protocol may be recommended when a Promax 3D CBCT examination is required for assessment of a patient's TMJ.

## Acknowledgment

The authors express their sincere appreciations to the dentists who assessed all the test radiographs.

## References

- Westesson PL, Katzberg RW, Tallents RH, Sanchez-Woodworth RE, Svensson SA. CT and MR of the temporomandibular joint: comparison with autopsy specimens. *AJR Am J Roentgenol* 1987; **148**: 1165–1171.
- Manzione JV, Katzberg RW, Brodsky GL, Seltzer SE, Mellins HZ. Internal derangements of the temporomandibular joint: diagnosis by direct sagittal computed tomography. *Radiology* 1984; **150**: 111–115.
- Pauwels R, Beinsberger J, Collaert B, Theodorakou C, Rogers J, Walker A, *et al*. Effective dose range for dental cone beam computed tomography scanners. *Eur J Radiol* 2012; **81**: 267–271.
- Araki K, Maki K, Seki K, Sakamaki K, Harata Y, Sakaino R, *et al*. Characteristics of a newly developed dentomaxillofacial X-ray cone beam CT scanner (CB MercuRay): system configuration and physical properties. *Dentomaxillofac Radiol* 2004; **33**: 51–59.
- Cheng JG, Zhang ZL, Wang XY, Zhang ZY, Ma XC, Li G. Detection accuracy of proximal caries by phosphor plate and cone-beam computerized tomography images scanned with different resolutions. *Clin Oral Investig* 2012; **16**: 1015–1021.
- Ghaemnia H, Meijer GJ, Soehardi A, Borstlap WA, Mulder J, Berge SJ. Position of the impacted third molar in relation to the mandibular canal. Diagnostic accuracy of cone beam computed tomography compared with panoramic radiography. *Int J Oral Maxillofac Surg* 2009; **38**: 964–971.
- Matherne RP, Angelopoulos C, Kulild JC, Tira D. Use of cone-beam computed tomography to identify root canal systems in vitro. *J Endod* 2008; **34**: 87–89.
- Holberg C, Steinhäuser S, Geis P, Rudzki-Janson I. Cone-beam computed tomography in orthodontics: benefits and limitations. *J Orofac Orthop* 2005; **66**: 434–444.
- Hatcher DC, Dial C, Mayorga C. Cone beam CT for pre-surgical assessment of implant sites. *J Calif Dent Assoc* 2003; **31**: 825–833.
- Dos Anjos Pontual ML, Freire JS, Barbosa JM, Frazao MA, Dos Anjos Pontual A. Evaluation of bone changes in the temporomandibular joint using cone beam CT. *Dentomaxillofac Radiol* 2012; **41**: 24–29.
- Librizzi ZT, Tadinada AS, Valiyaparambil JV, Lurie AG, Mallya SM. Cone-beam computed tomography to detect erosions of the temporomandibular joint: effect of field of view and voxel size on diagnostic efficacy and effective dose. *Am J Orthod Dentofacial Orthop* 2011; **140**: e25–e30.
- Honda K, Larheim TA, Maruhashi K, Matsumoto K, Iwai K. Osseous abnormalities of the mandibular condyle: diagnostic reliability of cone beam computed tomography compared with helical computed tomography based on an autopsy material. *Dentomaxillofac Radiol* 2006; **35**: 152–157.
- Tsiklakis K, Syriopoulos K, Stamatakis HC. Radiographic examination of the temporomandibular joint using cone beam computed tomography. *Dentomaxillofac Radiol* 2004; **33**: 196–201.
- Zain-Alabdeen EH, Alsadhan RI. A comparative study of accuracy of detection of surface osseous changes in the temporomandibular joint using multidetector CT and cone beam CT. *Dentomaxillofac Radiol* 2012; **41**: 185–191.
- Katakami K, Shimoda S, Kobayashi K, Kawasaki K. Histological investigation of osseous changes of mandibular condyles with backscattered electron images. *Dentomaxillofac Radiol* 2008; **37**: 330–339.
- Qu XM, Li G, Ludlow JB, Zhang ZY, Ma XC. Effective radiation dose of ProMax 3D cone-beam computerized tomography scanner with different dental protocols. *Oral Surg Oral Med Oral Pathol Oral Radiol Endod* 2010; **110**: 770–776.
- Zhang ZL, Cheng JG, Li G, Zhang JZ, Zhang ZY, Ma XC. Measurement accuracy of temporomandibular joint space in

- Promax 3-dimensional cone-beam computerized tomography images. *Oral Surg Oral Med Oral Pathol Oral Radiol Endod* 2012; **114**: 112–117.
18. Honey OB, Scarfe WC, Hilgers MJ. Accuracy of cone-beam computed tomography imaging of the temporomandibular joint: comparisons with panoramic radiology and linear tomography. *Am J Orthod Dentofacial Orthop* 2007; **132**: 429–438.
  19. Farronato G, Garagiola U, Carletti V, Cressoni P, Mercatali L, Farronato D. Change in condylar and mandibular morphology in juvenile idiopathic arthritis: cone beam volumetric imaging. *Minerva Stomatol* 2010; **59**: 519–534.
  20. Li G, Qu XM, Chen Y, Zhang J, Zhang ZY, Ma XC. Diagnostic accuracy of proximal caries by digital radiographs: an in vivo and in vitro comparative study. *Oral Surg Oral Med Oral Pathol Oral Radiol Endod* 2010; **109**: 463–467.
  21. Hintze H, Wenzel A. Clinical and laboratory radiographic caries diagnosis. A study of the same teeth. *Dentomaxillofac Radiol* 1996; **25**: 115–118.